



Degradation of historical paper induced by synchrotron X-ray technical examination

Alice Gimat · Sebastian Schöder ·
Mathieu Thoury · Anne-Laurence Dupont

Received: 23 October 2021 / Accepted: 23 March 2022 / Published online: 23 April 2022
© The Author(s), under exclusive licence to Springer Nature B.V. 2022

Abstract This research explores how intrinsic factors such as constituents and degradation state can impact the modifications incurred in aged papers during and after X-ray examination. To this end laboratory model papers, artificially aged, and eighteenth and nineteenth century archival documents, with and without additives (gelatin, calcium carbonate) and iron gallate ink, were exposed to Synchrotron X-ray radiation at doses commonly applied (7 Gy to 4 kGy). The threshold dose of 210 Gy previously shown to incur damage in unaged cotton papers falls in this range. Glycosidic scissions, hydroxyl free radicals, UV luminescence and yellowing were measured immediately after the irradiation, and were monitored

over a period of three years. Cellulose depolymerization was lower in the aged papers, as well as in the papers containing calcium carbonate and gelatin, than in the unaged fully cellulosic papers. Compared to the papers with no additives, there were more hydroxyl free radicals in the papers with calcium carbonate and slightly less in the gelatin sized papers. UV luminescence and yellowing both appeared post-irradiation, with a delay of several weeks to months. The papers with iron gallate ink showed limited degradation in the low doses range, most probably due to recombination of the free radicals produced. Doses below 4 kGy did not cause yellowing or UV luminescence of the archival papers within the whole monitoring period. The archival papers in good conservation state depolymerized to the same extent as the model papers, while the most degraded archival papers were less impacted than the latter.

Supplementary Information The online version contains supplementary material available at <https://doi.org/10.1007/s10570-022-04552-3>.

A. Gimat (✉) · A.-L. Dupont (✉)
Centre de Recherche Sur La Conservation Des Collections
(CRC, CNRS UAR 3224), Muséum National d'Histoire
Naturelle, 36 rue Geoffroy St Hilaire, 75005 Paris, France
e-mail: alice.gimat@mnhn.fr

A.-L. Dupont
e-mail: anne-laurence.dupont@mnhn.fr

S. Schöder
Synchrotron SOLEIL, 91192 Gif-sur-Yvette, France

M. Thoury
IPANEMA, CNRS, Ministère de la Culture, UVSQ, UAR
3461, Université Paris Saclay, 91192 Gif-sur-Yvette,
France

Keywords Calcium carbonate · Cellulose degree of polymerization · Gelatin · Iron gallate ink · Yellowing · UV fluorescence

Introduction

Because they are perceived as non-destructive, X-ray analytical techniques are commonly used to examine historic documents and artworks on paper and gain insight into their materials, manufacturing techniques and history (Creagh 2007; Albertin et al. 2015; IAEA

2016; Kozachuk et al. 2016; Pouyet et al. 2017). Because they are ionizing, X-rays induce changes in organic (as well as inorganic) materials, yet the potential damage to the artefacts is never considered. This is largely due to the fact that very little is known about the degradation incurred and the reactions involved. This lack of knowledge and awareness underlines the need to investigate the issue.

Among the few studies that tackle with this problem, some have shown cellulose depolymerization, oxidation and changes in the optical properties under X-ray exposures (Mantler and Klikovits 2004; Kozachuk et al. 2016; Gimat et al. 2020) as well as during yet gamma-ray irradiation (shorter wavelengths than X-rays) used for mold disinfection (Ershov 1998; Bouchard et al. 2006; Henniges et al. 2013; Bicchieri et al. 2016). Our recent results have shown that in quasi-pure cellulose paper, the impact of X-rays was proportional to the dose (Gimat et al. 2020). Due to the large diversity in the components and in the degradation state of historic cellulosic artefacts, the global impact of X-ray photons is however difficult to foresee, hence the rationale for the present study.

Paper is made of plant fibers, which besides cellulose, most often also contain other biopolymers such as hemicelluloses and lignin. Additives, fillers and sizing, are usually added to writing and drawing quality papers to enhance usability parameters: e.g. reduce water permeability, increase opacity and enhance brightness. In cultural heritage collections, such papers also often bear media such as inks and pigments. The materials and chemicals used are diverse. In ambient conservation conditions, a number of these additives can impact the paper degradation rate. For instance gelatin (Dupont 2003a) and alkaline minerals (Reissland 1999; Sequeira et al. 2006; Ahn et al. 2012; Poggi et al. 2016) have been shown to decrease the cellulose depolymerization rate, whereas transition metals in inks and pigments promote degradation by producing acids and free radicals (Selih et al. 2007; Potthast et al. 2008). If and how additives can impact the radiation-induced degradation of cellulosic paper is still unknown. The presence of absorbing elements, such as iron in the metal-gallate ink or calcium in the fillers could have a shielding effect and decrease the nominal X-ray dose, thereby lowering the degradation impact. Such a shielding effect could also be counteracted by the free radicals formed via the transition metals, which

are known cellulose degradation promoters (Emery and Schroeder 1974; Jeong et al. 2014). It has been shown that iron-containing pigments undergo a redox reaction under X-ray radiation (Bertrand et al. 2015; Gervais et al. 2015; Gimat 2016). Moreover, the structural modification of an additive under irradiation can also affect the paper degradation rate. For instance, X-rays were shown to produce defects inside calcium carbonate (Kabacińska et al. 2017), whereas polypeptide chains (e.g. gelatin) were shown to undergo hydrolysis (Moini et al. 2014). Bicchieri et al. have examined the combined impact of the degradation state and certain paper additives on the degradation incurred by ionizing radiation used for mold disinfection (Bicchieri et al. 2016). The authors used gamma-rays at a dose of 3 kGy. They tested cellulose paper Whatman n°1, as well as a commercial permanent paper (with CaCO₃ filler and optical brighteners, and sized with alkyl ketene dimers), which they pre-degraded by an acid treatment. The acid treated samples showed less radiation induced depolymerization than the Control samples, indicating that the degradation state played a role. The permanent paper yellowed more than Whatman n°1, which was attributed to structural modifications of calcium carbonate and optical brighteners under gamma radiation. To our knowledge, such study has not been conducted using X-rays, nor at lower doses used during synchrotron X-ray examination of cellulosic cultural heritage artefacts. This lack of research motivated the present study, which attempts at better understanding the mitigated impact of X-rays on paper, depending on the fiber deterioration level and on the presence of components other than the fibers.

Handmade linen rag papers from the eighteenth and nineteenth century and industrially-made cotton linters papers (Whatman n°1) to which various additives were incorporated (gelatin, calcium carbonate and iron gallate ink) were exposed to synchrotron X-ray radiation. The aim was (1) to study the impact of the photon energy and (2) reach high doses, similar to those used during spectroscopic examinations with instruments in such large-scale facilities. The papers, some of which had been previously artificially aged, were irradiated at doses in the range 0.007–4 kGy. The samples were characterized immediately after the exposure using a multiscale analytical procedure developed in a previous study (Gimat et al. 2020), which encompasses the macroscopic (yellowing and

UV luminescence) and the microscopic scales (glycosidic scissions and formation of hydroxyl radicals). The changes were monitored over a period of three years.

Materials and methods

Paper samples

Laboratory-prepared samples

Two types of paper were used: Whatman n°1 (W), which is a commercial paper made of cotton linters (min. 98% alpha cellulose), and a linen rag paper (R) manufactured using traditional stamper beating at Moulin du Verger papermill (Puymoyen, France). W and R were used either with no further modification (Control samples), or upon undergoing various artificial aging treatments (aged samples), in an attempt to approach the molecular degradation state of centuries old cultural heritage papers. Two artificial aging conditions, one predominantly hygrothermal (*hyg*) and the other predominantly oxidative (*ox*), were used to depolymerize and increase the carbonyl content of cellulose. The conditions were adjusted so as to achieve a similar degree of polymerization (*DP*) and a different degree of oxidation in the *hyg* and *ox* samples.

Hyg aging of W and R (samples called W_*hyg* and R_*hyg*) was performed according to the TAPPI method (T 573 sp-15 2015). Glass tubes (Wheaton, 35 mm internal diameter (ID) × 147 mm, 144 mL) were filled with 4.0 g of paper (dry weight), i.e. 4.23 g of paper conditioned at 50% relative humidity (RH) and 23 °C, based on the value of the equilibrium moisture content ($EMC = 5.43\%_{wt}$) determined with the sorption isotherm. The tubes were hermetically closed and heated at 100 °C in an oven (Memmert UN 55 oven) during 10 days to reach a decrease in *DP* of about 50%. During *hyg* aging, the relative humidity in the tube stabilizes around 50% thanks to the moisture contained in the paper so that both hydrolysis and oxidation occur. The weight-average degree of polymerization (*DP*_w) of cellulose was measured using SEC-MALS-DRI (details in Physico-chemical characterizations section) and the copper number (*N*_{Cu}) was determined using the standard method (T 430 cm-99 1999). The

total carbonyl groups concentration was derived from *N*_{Cu} using the following formula proposed by Röhring: $[CO] = \frac{(N_{Cu}-0.07)}{0.06}$ (Röhring et al. 2002). *DP*_w for W_*hyg* and R_*hyg* was $1490 \pm 2\%$ and $1961 \pm 1.6\%$, respectively. *N*_{Cu} of W_*hyg* was 0.11.

Oxidative degradation (*ox*) was carried out by immersing W in an aqueous solution of sodium hypochlorite (0.42–0.62% active chlorine) adjusted to pH 7 with HCl 6 N, during 15 min under gentle stirring. At this pH, NaClO is known to promote enhanced carbonyl groups formation (aldehyde, ketone, and carboxyl groups) on C2, C3 and C6, short chain organic acids as well as considerable glycosidic scissions (Nevell 1985). The samples (called W_*ox*) were abundantly rinsed with milli-Q water until neutral pH of the water, and were dried between blotters. The *DP*_w for W_*ox* was $1352 \pm 2\%$ and *N*_{Cu} was 0.42.

Some of the W_*ox* samples additionally underwent a reduction treatment with Na(BH)₄ to reduce the carbonyl groups produced during the aging (aldehyde and keton functions) to alcohol groups, and achieve a nearly null *N*_{Cu}. To this end, a solution made with anhydrous Na(BH)₄ (Sigma) (2.91 g) dissolved in absolute ethanol (154 mL) was prepared, in which 1.54 g of paper was immersed and left under gentle stirring during 12 h (Burgess 1988; Carter 1996). After reduction, the papers were abundantly rinsed with milli-Q water until the water reached neutral pH, and were dried between blotters. The samples were called W_*red*.

A portion of the W and R Control samples were sized by immersing the paper sheets in a 20 g L⁻¹ aqueous solution of type B photographic grade gelatin from cattle bone (Gelita type restoration 1, Kind & Knox) at 30 °C during 10 min. The sheets were then dried vertically at ambient temperature. The sized samples were named W_G and R_G.

The dry gelatin uptake (UP) of W_G and R_G, determined as $UP = \frac{m_{sized} - m_{unsized}}{m_{unsized}}$, was $4.8\% \pm 0.2$. Dry masses of the sized paper (*m*_{sized}) and of the unsized paper (*m*_{unsized}) were calculated subtracting the EMC at 23 °C and 50% RH measured according to the standard method (T 502 cm-07 1998). The UP value falls in the range of gelatin content in historical papers (Barrow 1972; Barrett 1992) and corresponds to a substantial amount of size in the paper (qualified as with ‘+’ in Table 1).

Table 1 Samples characteristics: constituents, aging method, thickness (x), equilibrium moisture content (EMC) at 23 °C and 50% RH (T 502 cm-07 1998), weight-average or viscometric-average (denoted *) degree of polymerization (DP_0), pH (T 509 om-15 2002), copper number (N_{Cu}) (T 430 cm-99 1999), concentration of total carbonyl groups ([CO]) (Röhring et al. 2002), ash content (measured at 525 °C) (T 211 om-02 2002), alkaline reserve (AR) expressed as % $CaCO_3$ (T 553 om-00 2000). Standard deviation (STD) is provided when possible.

Cot: cotton papers; lin: linen rag pulp papers; ox: oxidative degradation; hyg: hygrothermal aging; red: reduction treatment; nat. natural aging; Ca: calcium carbonate filler; I: iron gallate ink; G: gelatin sizing (identified with hydroxyproline spot test, with ++: highest size content; +: medium size content; -: lowest size content (levels defined with a water drop absorption test) (Fig. S4 in the Supplementary data file). n.d. stands for not determined

Sample	Fiber	Additive	Aging	x (μm)	EMC (% wt)	DP_0	pH	$N_{Cu}/[CO]$ ($\mu\text{mol g}^{-1}$)	Ash (%)	AR (%eq)
W	Cot	None	None	170	5.43 ± 0.02	$2948 \pm 2\%$	6.90 ± 0.02	0.05	< 0.1	
W_hyg	Cot	None	Hyg	151	5.46	$1490 \pm 2\%$	6.2 ± 0.2	0.11/0.67		
W_ox	Cot	None	Ox	170	n.d.	$1352 \pm 2\%$	6.73 ± 0.02	0.42/5.83		
W_red	Cot	None	Ox/red	170	n.d.	$1431 \pm 1.1\%$	6.41 ± 0.05	0.02		
W_G	Cot	G+	None	170	6.13	$3021 \pm 1\%$	5.70			
W_GI	Cot	G+, I	None	170	6.90	2225*	4.21			
K	Cot	Ca	None	100	5.61	$2566 \pm 2\%$	8.89		7.6	7.3
W_Ca	Cot	Ca	None	170	5.20	$2803 \pm 2.2\%$	8.86		5.4	6.0
R	Lin	None	None	160	5.78 ± 0.18	2980	7.90			
R_hyg	Lin	None	Hyg	141	6.14	$1961 \pm 1.6\%$	7.55			
R_G	Lin	G+	None	160	6.57	$3326 \pm 6.8\%$	7.68			
R_GI	Lin	G+, I	None	150	7.21	2290*	5.15			
SE	Lin	G~	Nat	115	5.46	$1000 \pm 9.4\%$	5.90			
LN5	Lin	G++	Nat	125	5.36	$1039 \pm 5.7\%$	4.92		1.1	
M	Lin	G++	Nat	125	5.75 ± 0.04	$1490 \pm 12.8\%$	5.03		1.5	
M_I	Lin	G+++, I	Nat	125	n.d.	702*	n.d			
LN1	Lin	G+	Nat	165	5.12	$1608 \pm 2.3\%$	5.28		0.8	
DCN	Lin	G~, Ca	Nat	90	6.01	$2869 \pm 6.2\%$	7.61		2.5	

Some of the W_G and R_G samples were used to apply the second compound of interest: iron gallate ink, also referred to as I (samples called W_GI and R_GI). The ink was prepared by mixing $FeSO_4 \cdot 7H_2O$ (Sigma Aldrich, 99%) (40 g L^{-1}), gallic acid monohydrate (Sigma Aldrich, 99%) (9 g L^{-1}) and gum Arabic (Sigma Aldrich, G9752) (140 g L^{-1}). The mixture was stirred during 3 days at room temperature. The amount of gum Arabic used was purposely high in order to limit the penetration of the ink inside the paper. The iron sulfate vs gallic acid ratio was adapted from a recipe used in previous work (Rouchon et al. 2011). Large inked strokes (1.5 cm wide each) were applied side by side with a flat-end metal pen (“Plakat”, Brause) in order to cover the whole sample surface. This procedure was not intended to replicate a quill pen stroke, but to provide a large and homogeneous inked surface ($2 \times 1 \text{ cm}^2$). The ink penetrated

30 to 112 microns into the paper, *i.e.* one third to one half of the sheet thickness, as observed with the optical microscope (Fig. S1 in the Supplementary data file). The iron content determined by XRF using a previously established calibration curve (unpublished data) was similar in both samples: $97 (\pm 5) \mu\text{mol g}^{-1}$ in W_GI and $110 (\pm 15) \mu\text{mol g}^{-1}$ in R_GI, values that are comparable to those in historical documents ($36\text{--}179 \mu\text{mol g}^{-1}$) (Rouchon et al. 2011).

The third compound added to the papers was $CaCO_3$ (samples called W_Ca). W paper was immersed in a saturated aqueous solution of calcium hydroxide (95%, Sigma Aldrich) (approx. 1.4 gL^{-1}) during 1 h and was dried in ambient air. This was repeated four times successively in order to achieve a high calcium carbonate content. After each bath, the paper sheets were placed between two blotters, and the excess solution was removed by applying a

10 kg Cobb test metal roller once back and forth on the blotters. Then the sheets were dried under weight. The reaction of CO_2 with the air when the paper is removed from the solution converts $\text{Ca}(\text{OH})_2$ to CaCO_3 , so-called alkaline reserve (AR). The AR determined according to the standard method (T 553 om-00 2000) was $1.18 \pm 0.06 \text{ mol kg}^{-1}$, otherwise expressed as equivalent $6.0\% \pm 0.3$ in CaCO_3 . Additionally, a commercial permanent paper made of cotton linters, which contained 7.25% precipitated CaCO_3 (Krypton parchment, Spixel Inc, formerly Domtar), was used (samples named K). Because it was manually prepared, Ca distribution inside W_{Ca} was less homogeneous than in K paper (Fig. S2 in supplementary data file). All the samples were conditioned prior to use at 50% RH, 23 °C according to the standard method (T 402 sp-08 2013).

Archival papers

Five archival paper documents from the eighteenth and nineteenth century manufactured with linen rags were chosen. They were named DCN, SE, LN1, LN5, and M. They all contain gelatin size to different degree, varying from light to strong, and have different *DP* (Table 1 and Fig. S3 in the Supplementary data file). SE is a page from an eighteenth century printed volume and has a slightly brownish hue, which appears darker in the center inked area of the page, due to natural aging. DCN is a printed decree and has a very faint bluish hue. These two papers seem to have the lowest amount of sizing (Fig. S4 in the Supplementary data file). The three other documents (LN1, LN5 and M) are individual folios of notarial deed documents. M is a blank paper while both LN1 and LN5 are handwritten with iron gall ink. In SE, DCN, LN1 and LN5, only ink-free areas were used, in order to better compare with M. Additionally, to investigate the effect of the iron gall ink on ancient archival paper, the laboratory-made iron gall ink was applied to some of the M samples using large strokes as previously described for papers W_{GI} and R_{GI} , which yielded a homogeneous inked area (sample called M_{I}).

Synchrotron X-ray radiation exposures

The papers were cut into a few cm^2 samples, inserted in plastic photography slide frames, and heated for 2 h at 40 °C (Memmert UN 55 oven) for gentle moisture desorption. They were then placed 48 h in a climatic chamber at 23 °C and 50% RH for equilibrium moisture regain, after which they were sealed in LDPE plastic bags where silica gel ProSorb (Atlantis) was added so as to maintain 50% RH ($\pm 5\%$). The EMC (23 °C, 50% RH) of the papers was determined according to the TAPPI test method (T 502 cm-07 1998) (Table 1). No moisture leakage was recorded upon monitoring the RH inside the bags for at least 72 h prior to the synchrotron radiation (SR) experiment with a temperature/humidity logger (Ibutton® Hygrochron, Measurement Systems Ltd). The bags were themselves sealed with Escal® film also filled with silica gel to stabilize the RH to 50% for transportation from the laboratory to the synchrotron facility.

The irradiation was performed on the beamline PUMA (SOLEIL synchrotron, Saclay). A monochromatic beam ($2 \times 1 \text{ cm}^2$) from a double crystal monochromator (DCM) with Si(111) crystals was used at photon energies of 7.22 keV, 12.5 keV or 18 keV. The samples were exposed perpendicular to the beam, inside the LDPE bags. The irradiation duration varied to reach various doses in the range 7 Gy to 4 kGy. The dose *D* (Gy) is defined as the total energy deposited per mass unit of material. As it is not possible to directly measure it via dosimetric techniques, which would be of limited accuracy in a heterogeneous material such as paper, it was calculated as follows:

$$D = \frac{F \cdot E \cdot t}{m} = \frac{I_0 \cdot (1 - e^{-\mu \cdot x}) \cdot E \cdot t}{\rho \cdot \sigma \cdot x}$$

with *F*, the absorbed photon flux (ph s^{-1}); *E*, the energy of X-ray photons (J); *t*, the exposure time (s); I_0 , the incident flux (ph s^{-1}); *m*, the mass of paper (kg); *x*, the thickness of paper (cm); ρ its density (g cm^{-3}); σ , the beam imprint; μ the linear attenuation coefficient (cm^{-1}), which was determined by measuring the incident and transmitted flux impinging stacked sheets as previously described (Gimat et al.

2020). The dose rate was obtained by the ratio D over the exposure time. For Whatman paper n°1, the dose rate was 0.71 Gy s^{-1} at 7.22 keV and 18 keV and 1.35 Gy s^{-1} at 12.5 keV.

Physico-chemical characterizations

After the irradiation, the samples were kept in the dark at 50% RH and 23 °C until analysis. The analyses were usually performed within 6 days, the latter being the shortest possible duration between the irradiation and the analysis. This allowed for immediate damage assessment. Post-irradiation monitoring was carried out by regularly re-examining the samples.

Molar masses

The molar mass distribution and the number- and weight-average molar masses of cellulose M_n and M_w were determined using Size-Exclusion Chromatography (SEC), except for the inked samples which were analyzed using viscometry. For SEC, paper samples (3–5 mg) were prepared and analyzed as described previously (Dupont 2003b). The precision on M_w was between 0.2 and 4.0 RSD%, depending on the samples.

S , the glycosidic scissions concentration, was calculated using DP_n , with $DP_n = \frac{M_n}{M_{AGU}} = \frac{N_{AGU}}{N_{molecule_t}}$, where N_{AGU} is the total number of anhydroglucose units, i.e. monomers ($M_{AGU} = 162 \text{ g mol}^{-1}$) and $N_{molecule_t}$ is the total number of cellulose molecules at any time t (μmoles). As each glycosidic bond scission increases by one the number of cellulose chains, the increase in the concentration of new chains formed is equal to S . The number of scissions being equal to $N_{molecule_t} - N_{molecule_{t_0}}$ and N_{AGU} being equal to $6170 \mu \text{ mol g}^{-1}$ of paper, hence $S = 6170 \left(\frac{1}{DP_{n_t}} - \frac{1}{DP_{n_{t_0}}} \right) \mu\text{moles g}^{-1}_{\text{paper}}$ (Whitmore and Bogaard 1994).

In order to avoid polluting the SEC columns with iron, DP of the gelatin-ink coated samples W_GI and R_GI was measured using viscometry in cupriethylene diamine (CED) (T 230 om-19 1999) with a capillary viscometer Routine 100 (Cannon–Fenske). Irradiation was carried out four days after the ink

application. Due to experimental constraints, the viscometry measurements were carried out 29 days after the irradiation. Before the viscometry analysis, the paper samples were chemically reduced with NaBH_4 (same treatment as described above) in order to avoid solvent induced depolymerization. They were dried between blotters and conditioned at 50% RH and 23 °C. The viscometric DP (DP_v) was calculated from the intrinsic viscosity $[\eta]$ using the Mark-Houwink-Sakurada equation, by applying the coefficients proposed by Evans and Wallis (Evans and Wallis 1987): $[\eta] = 0.91 \times DP_v^{0.85}$. DP_v is assumed to be very close to DP_w as M_v has been reported to be closer from M_w than M_n (Ross-Murphy 1985). This allows to parallel DP_v with DP_w with some confidence. The formula proposed by Dupont et al. (Dupont et al. 2018) was used for the conversion of DP_v to DP_n : $DP_n = 1575e^{(DP_w/3536)} - 1575$.

Hydroxyl radicals

The paper samples were soaked for 3 min in a methanolic solution of terephthalic acid (TPA) (98%, Sigma Aldrich) (1 mM). They were left to dry at ambient temperature for 24 h and conditioned at 23 °C at 50% RH. TPA reacts with hydroxyl free radicals (HO^\bullet) in the paper and produces hydroxyterephthalic acid (HTPA), which accumulates in the paper. HTPA was extracted from the paper (2–3 mg) by soaking during three hours in 300 μl of phosphate buffer (KH_2PO_4 50 mM pH 3.2, 70% water:30% methanol), and was quantified by reverse phase liquid chromatography with UV and fluorescence detection (RP-HPLC/FLD-DAD) according to a previously established method (Jeong et al. 2014). HTPA ($\mu\text{mol g}^{-1}$) was calculated with respect to the paper dry weight, subtracting the additives weight, to correlate sample behavior based on their cellulosic content only. In order to ensure the quality of the results, it was verified that no HTPA was formed upon irradiating TPA powder.

Colorimetric and UV luminescence measurements

The diffuse reflectance and UV luminescence of the paper samples were measured with a non-invasive UV–Vis–NIR spectroradiometer (Specbos 1211UV, JETI). For UV luminescence, the excitation was centered at 365 nm (with full width half-maximum

FWHM=20 nm). Measurements were normalized to a blue luminescent certified reflectance standard (USFS-461 Spectralon) to correct for light intensity change with time. The maximum intensity of each UV luminescence spectrum was used to monitor the global intensity change. To calculate the change the following formula was used:

$$\Delta I(\lambda_{\max}) = I(\lambda_{\max})[irr] - I(\lambda_{\max})[Ctrl]$$

with $I(\lambda_{\max})[irr]$ and $I(\lambda_{\max})[Ctrl]$ the intensities of luminescence at the wavelength maxima measured inside (irr) and outside (Ctrl) of the irradiated area, respectively.

A spectrophotometer (Konica Minolta, CM-26d) was used to measure the chromaticity coordinates L^* , a^* and b^* in the CIELAB 1976 system. The variation of the color coordinate b^* , which spans on the blue-yellow scale, was used to quantify the yellowing expressed as $\Delta b^* = b^* - b_0^*$ (positive value).

Results and discussion

Calculation of the SR X-ray dose

The extent of radiation damage usually depends on the X-ray dose absorbed by a sample. Different papers are expected to absorb X-ray differently, especially when heavy elements are present as the latter increase the absorption. Defining the X-ray dose is thus essential in order to compare changes in paper samples after irradiation on a common basis. In order to do so, it is necessary to define the linear attenuation coefficient (μ) of each sample for each

experimental setup and condition. The value of μ was measured with the incident and transmitted flux impinging stacked sheets as previously described (Gimat et al. 2020). This value depends on the sample characteristics and on the X-ray energy. Indeed, μ decreases with increasing energy, mainly due to the decrease of photoelectric effect. The values of μ measured for W were: $4.29 \pm 0.07 \text{ cm}^{-1}$ at 7.22 keV, $1.02 \pm 0.06 \text{ cm}^{-1}$ at 12.5 keV and $0.32 \pm 0.031 \text{ cm}^{-1}$ at 18 keV. The values of μ for all the papers at 7.22 keV are given in Table 2. These values fell in the same range for the archival papers and the model papers. As expected, the values in the table show a positive variation of μ with the paper's density (ρ). Indeed, in denser papers the beam path crosses more absorbing atoms. A plot of μ vs ρ (Fig. S7 in Supplementary data file) shows that for all the papers the two values are actually strongly positively correlated, and that ρ explains most of the variation in μ , sometimes all the variation, depending on the samples. For instance, for gelatin sized papers (W_G, R_G), degraded model (W_hyg, W_ox and R_hyg) and archival papers, a higher μ compared to the Control samples was ascribable exclusively to a higher paper density. However, for some samples, there was an additional input to μ . This is the case for samples W_Ca and K, and was attributed to the presence of Ca. Ca is a heavy element and has a higher photon absorption than the atoms in cellulose. It was thus expected that Fe in the inked samples would have the same impact on μ when compared to the counterpart samples with no ink. This was indeed the case for R_GI and M_I, but not for W_GI (Fig. S7 in Supplementary data file).

Table 2 Linear attenuation coefficient μ (cm^{-1}) with standard deviation and density (ρ) of the studied papers at 7.22 keV, 50% RH

	Cotton papers		Linen rag papers		Archival papers (gelatin sized)			
	μ (cm^{-1})	ρ (g cm^{-3})	μ (cm^{-1})	ρ (g cm^{-3})	μ (cm^{-1})	ρ (g cm^{-3})		
W	4.29 ± 0.07	0.51	R	5.01 ± 0.25	0.54	LN5	5.60 ± 0.23	0.62
W_G	4.76 ± 0.02	0.54	R_G	4.77 ± 0.07	0.53	M	5.69 ± 0.03	0.47
W_GI	7.03 ± 0.04	0.62	R_GI	7.99 ± 0.08	0.55	M_I	10.05 ± 0.03	0.72
W_Ca	6.89 ± 0.12	0.54				SE	6.66 ± 0.04	0.64
K	9.56 ± 0.20	0.68				LN1	7.21 ± 0.10	0.68
W_hyg	5.32 ± 0.07	0.55	R_hyg	5.69 ± 0.28	0.60	DCN	8.18 ± 0.60	0.72
W_ox	5.66 ± 0.14	0.53						
W_red	5.28 ± 0.04	0.53						

DP and hydroxyl radicals

Impact of the X-ray dose and photon energy

All the X-ray radiation exposures were carried out on the PUMA beamline at synchrotron SOLEIL. Nevertheless, a first experiment, was carried out with a laboratory Micro X-ray Fluorescence Spectrometer (methodology in the Supplementary data file), to allow assessing the impact of low doses in the range of those usually delivered by these laboratory instruments. All the unaged W samples, irradiated to a dose up to 22 Gy, had a similar *DP* to the Control sample (Fig. S8 in the Supplementary data file), indicating that no macromolecular degradation took place during the irradiation, whether the dose was delivered at once or in several stages. This is consistent with the lowest observable adverse effect dose (LOAED) for glycosidic scissions of 0.21 kGy defined in our previous work (Gimat et al. 2020).

Synchrotron X-ray fluorescence experiments usually use energies in the range of 1 to 20 keV (Glaser and Deckers 2014), sometimes even higher if heavy elements are investigated. To investigate if the degradation was energy dependent, W samples were exposed to three photon energies: 7.22, 12.5 and 18 keV. Figure 1 shows the glycosidic scissions concentration (*S*) as a function of the absorbed dose up to 3.9 kGy, at the three energy levels. *S* increased with the dose in the range of 0 to 6 $\mu\text{mol g}^{-1}$. The

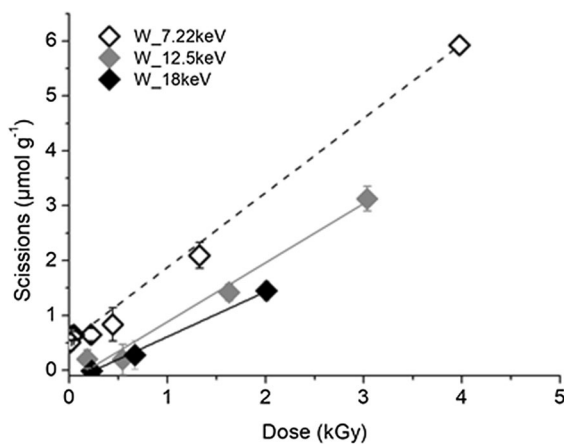


Fig. 1 Glycosidic scissions concentration *S* as a function of the X-ray dose in Whatman n°1 irradiated at energy of 7.22, 12.5 and 18 keV at 50% RH

impact was very small below the LOAED (0.21 kGy) and was followed by a linear increase from 0.5 kGy upwards. *S* increased steeply, similarly at 12.5 keV and 18 keV. At 7.22 keV, all the values of *S* were shifted up. A similar energy dependence has been observed for electron beam irradiation (Bouchard et al. 2006) at energies of several MeV. While the photoelectrons created by the X-ray photons in our experiment have much lower energies, it seems like the inverse relation between kinetic energy and cellulose damage remains true in the keV regime. We are not sure why this is the case, but it is noteworthy that the inelastic mean free path (IMFP) varies considerably for electron energies in the range of our experiment compared to the typical average diameter of cellulose fibers. The IMFP for electrons in graphite changes from 9.2 nm at 7.3 keV to 19.5 nm at 18 keV (Shinotsuka et al. 2015). While the exact path lengths in cellulose will likely be slightly different, this shows that it is thus much more probable that a photoelectron produced by 18 keV X-rays escapes the cellulose fibers before causing damage than it is for one produced by 7.22 keV X-rays. Although a lower dose rate can sometime increase material damage (Adamo et al. 2001), this was not observed here since glycosidic scissions concentration was higher at 7.22 keV than at 18 keV at similar dose rate (0.7 Gy s⁻¹), yet it was intermediate at 12.5 keV at higher dose rate (1.35 Gy s⁻¹) (Fig. 1). Based on these results, all the following experiments were carried out at 7.22 keV, the most penalizing conditions, to enhance the chances of observing and characterizing damage.

Impact of calcium carbonate and gelatin

The glycosidic scissions and hydroxyl free radicals concentrations in the unaged papers, in the papers with calcium carbonate and in the papers with gelatin increased in a quasi linear fashion as a function of the X-ray dose, up to 6 $\mu\text{mol g}^{-1}$ for W and up to 8 $\mu\text{mol g}^{-1}$ for R (Figs. 2 and 3). *S* in W_G was slightly lower than in W Control (Fig. 2a). This is consistent with the fact that gelatin size tends to lower the depolymerization rate of cellulose during the degradation induced by aging (Dupont 2003a). Besides gelatin, this could also be partly due to the difference in moisture in unsized vs sized paper (EMC at 23 °C of 5.43% and 6.13%, respectively), as moisture was shown to reduce cellulose depolymerization during synchrotron X-ray

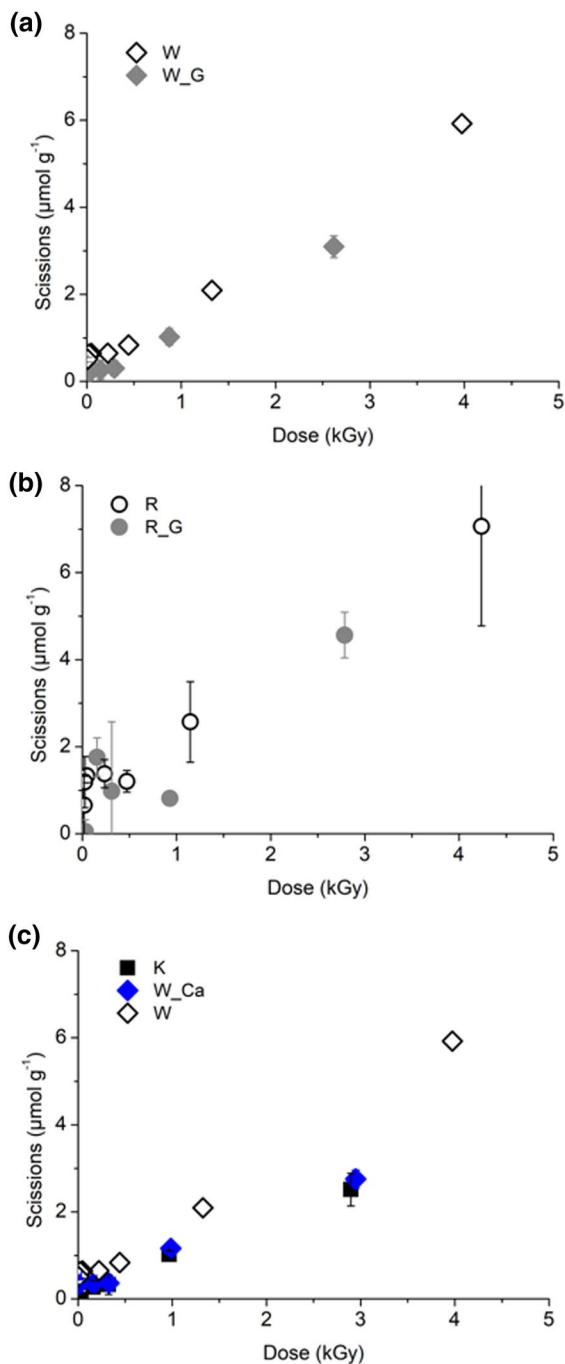


Fig. 2 Glycosidic scissions concentration (S) in W and R Control papers, papers with gelatin (W_G and R_G) (a, b) and with calcium carbonate (W_Ca and K) (c), as a function of X-ray dose after irradiation at 7.22 keV

irradiation (Gimat et al. 2020). Because of a larger standard deviation on the data points, this was less clearly established for R and R_G, where S values were

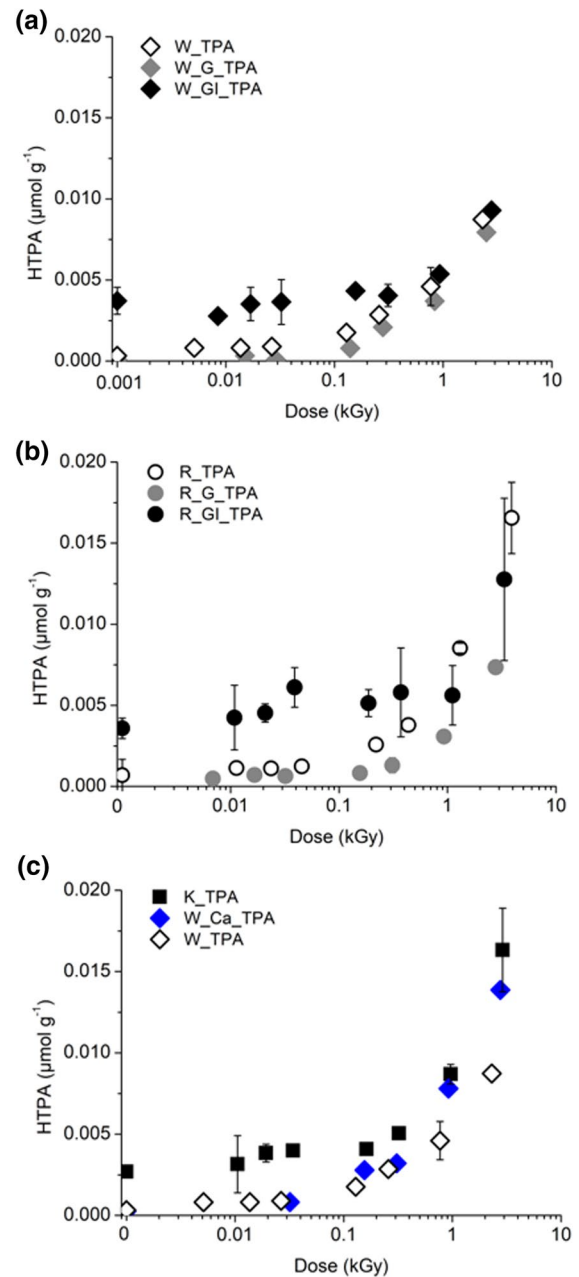


Fig. 3 Impact of gelatin, iron gallate ink (a, b) and calcium carbonate (c) in W and R papers on the HTPA concentration as a function of X-ray dose after irradiation at 7.22 keV. The logarithmic scale is used for easier visualization

quasi similar (Fig. 2b) despite the EMC difference (5.78% vs 6.57%, respectively) (Table 1).

The samples with gelatin (W_G and R_G) produced less hydroxyl radicals than the Control samples

(Fig. 3a, b). This could be an indication that gelatin was able to scavenge the HO^\bullet produced during the irradiation.

In both W_Ca and K, S increased slightly less as a function of the dose than in W Control, which is especially visible at the high doses, as shown on Fig. 2c. this suggests that calcium carbonate can buffer the organic acids generated by cellulose degradation caused by the X-ray exposure, which is the expected role of the alkaline reserve in paper (Whitmore and Bogaard 1994; Ahn et al. 2013; Rouchon and Belhadj 2016). On the other hand, W_Ca and K showed a larger HO^\bullet production than the Control samples (Fig. 3c). This, again, could be due to the pH, as an alkaline medium is known to enhance the lifetime of HO^\bullet radicals, and hence the probability that they react with TPA. These results also confirmed previous observations that the HO^\bullet concentration did not always correlate directly with the glycosidic scissions concentration, and indicate that other species and mechanisms are involved (Jeong et al. 2014; Gimat et al. 2020).

Impact of the iron gallate ink

For the three samples coated with the iron gallate ink (W_GI, R_GI and M_I), the DP of the non-irradiated samples was considerably lower than that of the Control samples (W, R and M) is represented by the arrows on Fig. 4. This was attributed to strong and almost instant acid hydrolysis and oxidation reactions due to the presence of iron gallate ink, which occurs within the period between sample preparation and analysis (33 days). This has been observed previously (Rouchon et al. 2011, 2016). Indeed, a DP loss of 25% and 30% was measured for W_GI and R_GI, respectively, which is consistent with previous observations (Rouchon et al. 2011) for inked Whatman n° 1 where a 24% DP loss was recorded within a similar timeframe. For M_I samples, the DP loss was 50%. A striking observation was made in the low doses range: after irradiation (up to 0.29 kGy for W_GI, 0.36 kGy for R_GI and 2.4 kGy M_I), the DP of the iron gallate ink coated samples was higher than the DP of their non-irradiated counterpart (Fig. 4, dashed lines). This is the reason why DP is represented instead of glycosidic scissions as y-axis on Fig. 4. This was interpreted as having two possible causes. First, it has

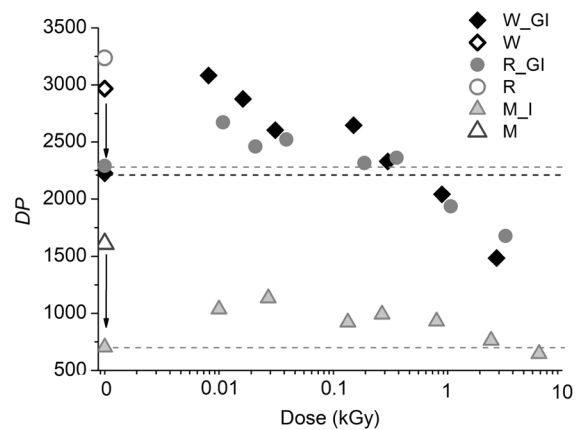


Fig. 4 Viscometric-average degree of polymerization (DP_v) of iron gallate ink coated papers W_GI (a), R_GI (b), and M_I (c) as a function of X-ray dose (kGy) after irradiation at 7.22 keV. The dose is represented on a logarithmic scale for easier visualization. Control samples without ink or gelatin are represented by the void data points. Arrows represent the DP drop due to the iron gallate ink. At low X-ray doses, irradiated samples have a higher DP than non-irradiated Control sample (above the dotted lines)

been shown that iron gallate ink containing papers produce free radicals, such as HO^\bullet and other reactive oxygen species (Gimat et al. 2016, 2017). This enhances the chances for free radicals recombination leading to the auto-oxidation termination reactions, and in turn would lower the concentration of radicals accumulated in the paper, thus, possibly preserving cellulose from their attack. Conversely in the Control samples, unexposed to X-rays, the free radicals would induce a higher level of degradation. Secondly, the crosslinking induced by the recombination of cellulosic radicals could lead to an increase in DP which would be measurable if the radicals have a relatively high molar mass. This is consistent with the fact that in the low irradiation doses range, HTPA was produced in higher amount in the irradiated ink coated samples W_GI and R_GI than in the Control counterparts W and R (Fig. 3a, b), and in similar amount as in non-irradiated W_GI and R_GI. In the higher doses range (from 0.89 kGy for W_GI, 1.1 kGy for R_GI, and 6.3 kGy for M_I), the samples reached a lower DP than the non-irradiated samples, and the HTPA concentration in the samples reached similar levels with and without ink. This was interpreted as an indication that the enhanced scissions induced by

the irradiation at the high doses likely exceeded the supposed impact of the free radicals recombination reactions.

Impact of the degradation state

The artificially degraded papers (W_{hyg} , W_{ox} and W_{red}) were irradiated at 7.22 keV to various doses to study if and how the degradation state modifies the impact of the X-rays exposure. The intent was to possibly extrapolate the results to centuries-old cultural heritage paper. The three samples had a similar starting DP ($DP_w \approx 1400$, *i.e.* about 50% lower than W) and a different oxidation state: $N_{Cu} = 0.42$ for W_{ox} (*i.e.* $5.83 \mu\text{mol g}^{-1}$ total carbonyl groups, as calculated according to (Röhring et al. 2002), $N_{Cu} = 0.11$ for W_{hyg} (*i.e.* $0.67 \mu\text{mol g}^{-1}$ total carbonyl groups) and $N_{Cu} = 0.02$ for W_{red} (*i.e.* near-zero carbonyl groups besides the reducing ends) (Table 1). Figures 5a, b show the glycosidic scissions concentration in these samples as a function of the dose. In W_{hyg} , S increased linearly with the dose, yet slightly less than in W Control (Fig. 5a). This suggests that lower DP and/or higher carbonyl groups concentration might lessen somewhat the impact of X-rays (Fig. S7 in the Supplementary data file). For samples that underwent oxidation (W_{ox} and W_{red}), S was in the same range (up to $6 \mu\text{mol g}^{-1}$) as for W and W_{hyg} at respective doses (Fig. 5b), yet with higher standard deviations. The main contrast between the two samples is in the low dose region. In the range –up to 0.5 kGy, while W_{red} underwent fewer glycosidic scissions, in W_{ox} S was higher than in the other samples, with a sharp increase to $1\text{--}2 \mu\text{mol g}^{-1}$ for doses below 1.4 kGy. This tends to indicate that at low doses, a high concentration of carbonyl groups in the paper may enhance the X-ray induced depolymerization. In the higher doses range (≥ 1 kGy), the depolymerization of all the samples reached the same range, between 4 and $6 \mu\text{mol g}^{-1}$. Figure 6a shows that a similar amount of HO^\bullet free radicals was produced in W_{hyg} and in W , indicating that the free radicals were not fully responsible for the difference in the glycosidic scissions, and that the HO^\bullet were not significantly involved in the production of carbonyl groups.

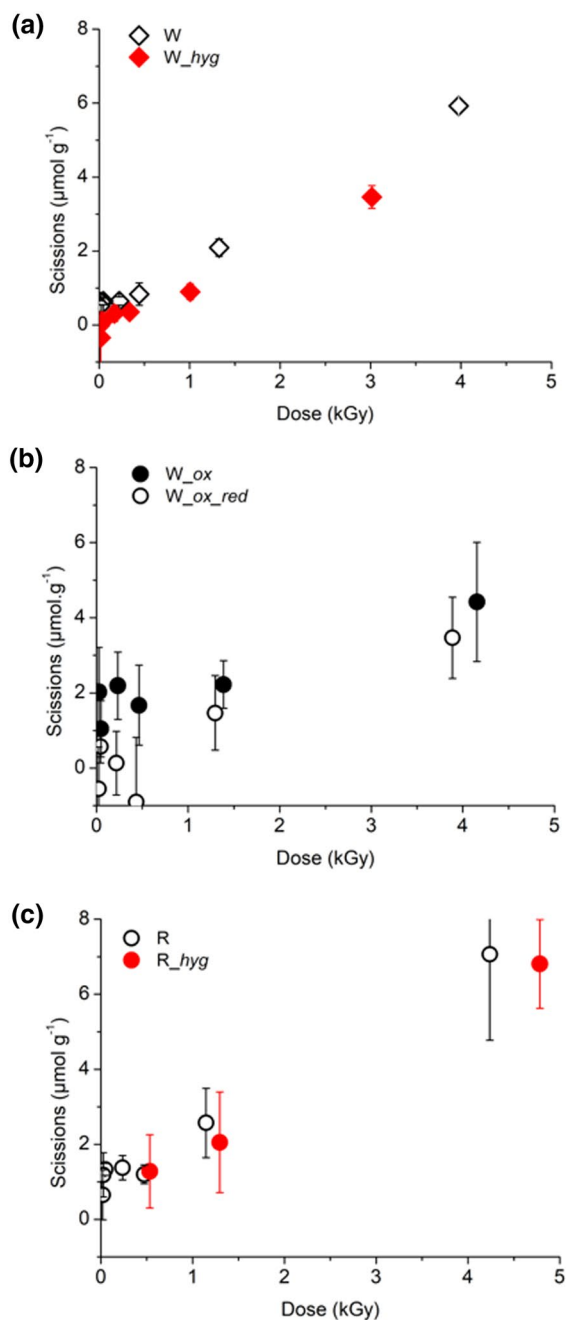


Fig. 5 Glycosidic scissions concentration (S) in aged papers W (a, b) and aged rag papers R (c) as a function of X-ray dose compared to respective Control samples

The results for the linen rag model papers are more difficult to interpret. S extended higher (up to $8 \mu\text{mol g}^{-1}$) and increased linearly as a function of the dose, yet, in a similar way for the undegraded

Control sample and for the degraded R_{hyg} , despite the DP of the latter being 34% lower ($DP_w \approx 1961$) (Fig. 5c). Moreover, above 0.1 kGy, slightly less HO^\bullet free radicals were detected in R_{hyg} than in R (Fig. 6b). This, and the large standard deviations on each data point of R samples muddles the interpretations. The extrapolation of the results from a simple machine-made cellulosic paper to a traditional handmade rag pulp paper is not straightforward. The next level of complexity, which was to test the response of archival papers, was thus anticipated as very challenging.

Archival paper documents

For the historic samples irradiated to various doses, S values were overall in the same range as those measured for the model samples. Only LN5 degraded

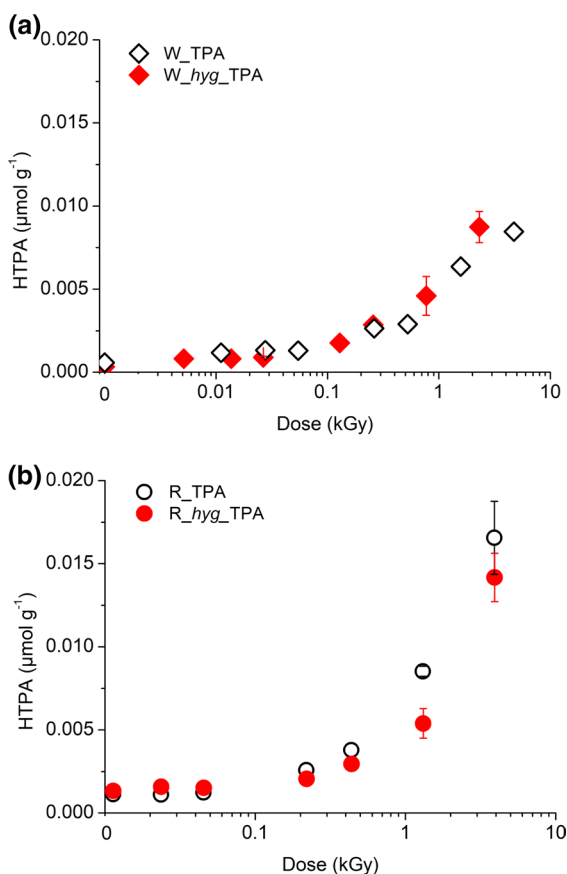


Fig. 6 HTPA concentration in Control samples, aged W (a) and aged R (b) as a function of X-ray dose

more and showed S values at least twice as high as for the other archival papers at all the doses tested (Figs. 7a, b). However, the depolymerization behavior with increasing dose was not progressive as observed for the model papers (except for LN1), especially in the low doses. For instance, SE did not undergo scissions below 3 kGy, and M had a constant degradation (plateau) response on the whole dose range, with S around $3.5 \mu\text{mol g}^{-1}$ (Fig. 7a). No correlation could be made with the DP (Table 1), or the paper constituents. All the papers have similar iron and calcium content, except maybe DCN which has more calcium due to the calcium carbonate filler and slightly more Fe (Fig. S6 in the Supplementary data file). The other possible difference in composition would be the gelatin content, the latter being a factor that tends to lower the degradation in the model papers. Unfortunately, the gelatin content of the archival papers was unknown and could not be measured. However, an indirect indication of sizing was given by a water drop absorption test, which showed that M and LN5 were more hydrophobic than DCN (Fig. S4 in the Supplementary data file). Even though there can be other reasons for paper hydrophobicity such as reduced porosity for instance, the former two showed higher S than the latter, which would tend to invalidate the aforementioned protective role of gelatin. The differences in S could thus arise from local heterogeneity and to samples' structural parameters such as porosity or constituents' composition. This was not unexpected as in handmade papers the additives are usually not as homogeneously distributed at the microscopic level as in industrial papers.

Very high doses, between 32 and 38 kGy, were then tested on the archival papers, as well as on W. The results showed that DCN, LN1 and LN5 were similarly extensively degraded as W, with S comprised between 30 and $43 \mu\text{mol g}^{-1}$ (Figs. 7a, b). M and SE resisted surprisingly well, being the least degraded samples, with S close to $10 \mu\text{mol g}^{-1}$. Despite the different kinetics, most samples approached LODP (Levelling Off Degree of Polymerization) with DP_w W=345; DP_w M=318; DP_w LN5=426; DP_w LN1=495. The least degraded samples were DCN ($DP_w=530$) and SE ($DP_w=708$) (Fig. 7c). The production of HO^\bullet free radicals was measured in SE and M. In SE, HO^\bullet concentration was very low, but it was higher in M over the whole dose range reaching a similar amount as in the model

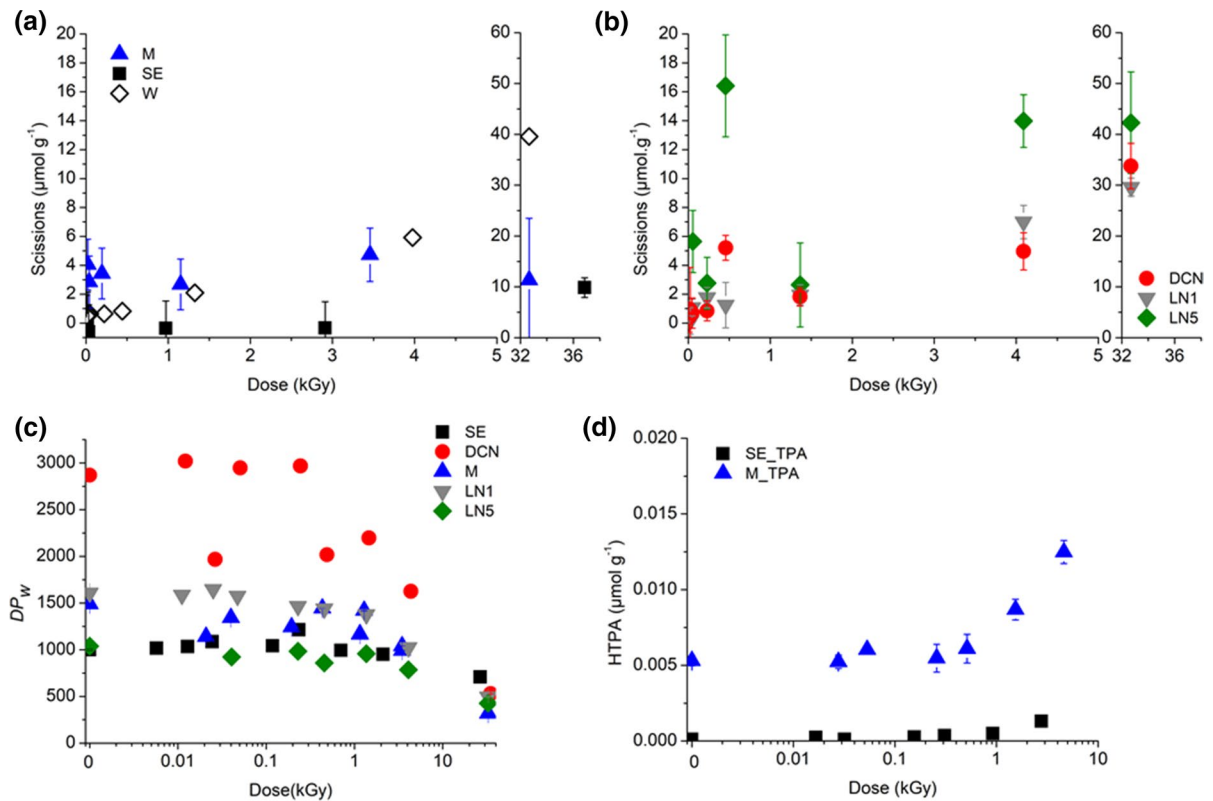


Fig. 7 Glycosidic scissions concentration (S) (a, b), DP_w (c) and HTPA concentration (d) in archival samples as a function of X-ray dose. Logarithmic scale c-d is used only for a better display of the data

papers containing Ca and Fe (Fig. 7d). This difference was thus attributed to the slightly higher calcium and iron content in M than in SE (Fig. S6 in the Supplementary data file).

UV Luminescence and yellowing

Before the irradiation, all the samples, model and archival, exhibited luminescence under UV when excited at 365 nm, which is a common feature of paper (Fig. S9 in the Supplementary data file). The model samples W and R exhibited a luminescence maximum λ_{\max} at 432 nm, which is consistent with previous data (Gimat et al. 2020). The intensity varied depending on the type of additive and on the degradation state, luminophores being produced during the aging. For instance gelatin is expected to show a broad luminescence spectrum with $\lambda_{\max} = 402$ nm (unaged) and 414 nm (artificially aged at 50% RH and 80° C) (Yova et al. 2001; Duconseille et al. 2016).

After X-ray exposure, no change in the UV luminescence spectral distribution was observed during the three years monitoring period. The intensity at λ_{\max} [$I(\lambda_{\max})$] of each spectrum was followed over time. After eight months, the area of the model papers irradiated at 7.22 keV (dose range from 2.8 to 4 kGy, depending on the sample) exhibited an increase in the intensity of the UV luminescence compared to the respective Control samples ($\Delta I(\lambda_{\max})$), as shown Fig. 8 and Fig. S10 (Supplementary data file). All Whatman n° 1 model papers (except for the sized samples), showed luminescence proportionally to the absorbed dose (Fig. 8, white marks, linear trendline). The highest increase in luminescence was observed on the sized samples W_G and R_G with $\Delta I(\lambda_{\max})_{R_G}$ of 0.0042 and $\Delta I(\lambda_{\max})_{W_G}$ of 0.0036 (R_G data not shown), indicating that a large quantity of luminophores was produced post-irradiation. These samples were still the most luminescent samples after 11 months. The luminescence of W_hyg and

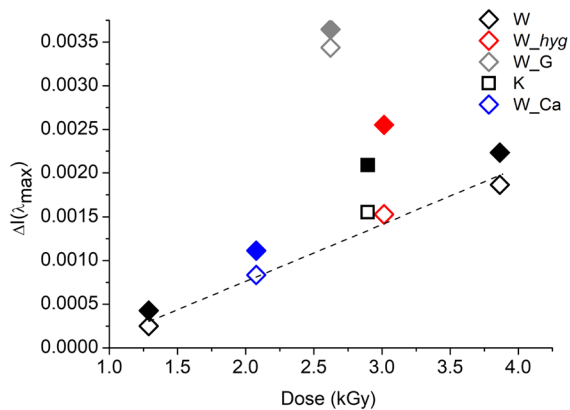


Fig. 8 $\Delta I(\lambda_{\max})$ of W, 8 months (empty marks) and 11 months (full marks) after X-ray irradiation. $\Delta I(\lambda_{\max})$ is the subtraction of the luminescence of the non-irradiated area from that of the irradiated area. The trendline represents the dose/luminescence response in W Ctrl samples

K grew beyond that of the other samples between 8 and 11 months. The change in luminescence between unaged and aged R papers (with no additives) was slower than for unaged and aged W, with a smaller $\Delta I(\lambda_{\max})$ of R and R_hyg (0.0011 and 0.00015, respectively) compared to W and W_hyg ($\Delta I(\lambda_{\max})$ (0.0022 and 0.0025, respectively).

Colorimetric measurements were carried out three years after the irradiation, on the irradiated areas and the non-irradiated Control samples (Fig. 9). All the model samples showed very small Δb^* values (Fig. 10a) and a global color change ΔE^* between 0.55 (for K) and 1.87 (for R), *i.e.* below the usually accepted level for a just noticeable difference. Among the W samples, the artificially aged W_hyg had the highest Δb^* (1.35 ± 0.26). The opposite trend was observed with R samples, where R_hyg had a lower Δb^* than R. This observed behavior difference is all the more valid since the data points for R on Fig. 10a correspond to higher doses than for W samples and that R_hyg is the most strongly irradiated sample. This may indicate complex radiochemistry mechanisms of chromophore destruction and chromogens formation. As opposed to the observations after hygrothermal aging of gelatin sized papers (Dupont 2003a; Missori et al. 2006), the irradiation did not modify the yellowing in the gelatin sized papers. This may be related to the radical scavenging properties of gelatin, which could lower the kinetics of cellulose

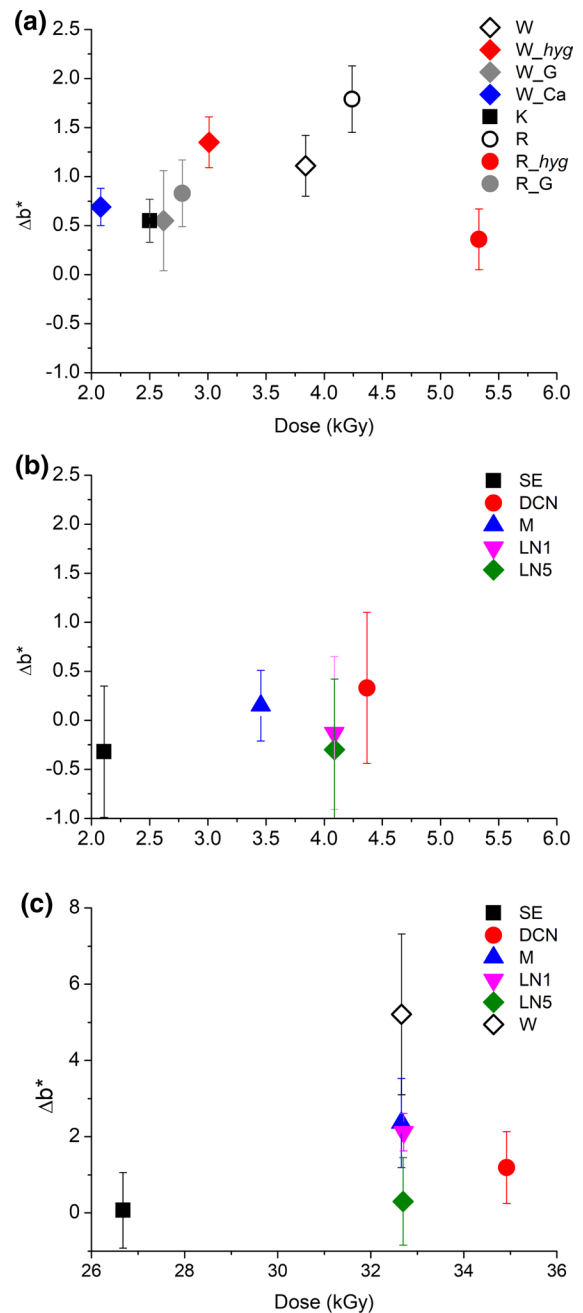


Fig. 9 Yellowing increase (Δb^*) of papers measured three years after X-ray irradiation at 7.22 keV depending on the dose for W and R model papers (a) and for the archival papers (b, c)

chromophores formation. To sum up, for the model samples, gelatin was the additive that had the highest impact on luminescence. This is most probably due to its own intrinsic luminescence properties and

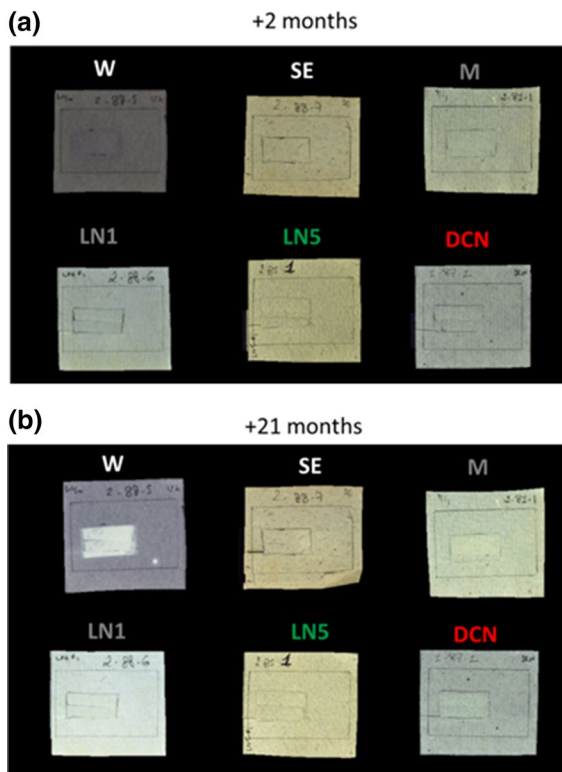


Fig. 10 Photographs under UV light of W and archival papers exposed to X-ray radiation at doses between 26 and 33 kGy, 1 month (a) and 21 months (b) after the irradiation at 7.22 keV

maybe also to its chromogenic degradation products appearing post-irradiation. Yellowing did not appear to be linked to either the initial degradation state nor to the presence of additives, which indicates complex mechanisms at play of chromogenic structure formation and destruction.

The initial UV luminescence spectra of the archival papers showed maxima with different intensities $I(\lambda_{\max})$ and positions (between 444 and 460 nm), which could be due to differences in the quantity and the type of UV-absorbing groups such as carbonyl compounds, respectively. This could also be due to a different moisture content, as the latter has been shown to affect the luminescence properties of paper (Kocar et al. 2005; Castellan et al. 2007). Before irradiation, no correlation between the state of degradation (DP) and the intensity of the luminescence of the papers could be made. Indeed, LN1 and M, both with similar DP around 1500, displayed more intense luminescence than the other historic samples,

either more degraded (DP_w LN5 = $1039 \pm 5.7\%$, and DP SE = $1000 \pm 9.4\%$) or less degraded (DP DCN = $2869 \pm 6.2\%$). The presence of gelatin could not be fully responsible of the luminescence intensity either, as the hydrophobic properties (indicating the gelatin content) did not correlate with luminescence (M and LN5 highly hydrophobic, LN1 medium hydrophobic, SE and DCN not hydrophobic).

After irradiation at doses below 4.4 kGy no change was observed on the archival papers. Indeed, no differences in the UV luminescence (data not shown) nor the yellowing ($\Delta b^* < 1$) were measured in the irradiated vs the non-irradiated areas (Fig. 9b). At the highest doses tested (26–36 kGy), a slight luminescence appeared on M and DCN twenty-one months after the irradiation (Fig. 10). It thus took almost two years for the luminophores to build up inside the archival papers. Similarly, as with the model samples, no correlation between the luminescence and the DP , or the glycosidic scissions could be made. A test was made by irradiating M at a very high dose (290 kGy), which induced marginal luminescence, and only after ten months (data not shown).

Within the high dose range (26–36 kGy), no change was observed for SE and LN5, and the other archival samples (DCN, M, LN1) exhibited a slight yellowing, with Δb^* of 1.2, 2.4, and 2.1, respectively (Fig. 9c). The strongest yellowing was recorded on W ($\Delta b^* = 5.2 \pm 2.1$).

Conclusion

Synchrotron X-ray radiation at energies and doses most often applied for analytical purposes to paper-based cultural heritage has been shown to be detrimental to one-component cellulosic paper (Whatman n°1). However, field situations are complex as historic papers are multiparametric, which interferes with a prediction of the effect of X-ray radiation. They usually are degraded to some extent and they contain other constituents besides biopolymers, such as papermaking additives, ink and their degradation by-products. The present research investigated how these parameters, when studied individually in model papers, could influence the X-ray radiation-induced degradation. The papers were artificially aged and/or supplemented with additives, which enabled to single

out some of the influential parameters. The additives tested were gelatin as sizing agent, and calcium carbonate as filler. Iron gallate ink was applied on some of the gelatin-sized papers, modeling writing/drawing medium. Following the same methodological approach as developed in a previous publication (Gimat et al 2020), the changes were measured immediately after the irradiation at the microscopic level (macromolecular and molecular degradation) and the macroscopic changes embodied by the optical properties (UV luminescence and yellowing) were monitored time-delayed.

In the dose range up to 4 kGy, gelatin-sized samples and samples with CaCO_3 underwent a slightly reduced irradiation-induced depolymerization. Surprisingly, up to 0.89–1.1 kGy, the iron gallate ink coated papers had a higher *DP* than the Control samples, which was attributed to a decrease in the impact of the free radical initiated autooxidation reactions through radicals recombination and crosslinking. Above these doses, a higher rate of scissions induced by the irradiation prevailed. The production of hydroxyl free radicals was higher in all the samples containing CaCO_3 , maybe due to the increased lifetime of HO^\bullet at alkaline pH. The depolymerization behavior of the aged model samples was different in the industrially-made (Whatman n° 1) and in the handmade papers (linen rags). Higher degradation state (lower *DP*) tended to stabilize Whatman n°1 paper towards X-ray radiation, by lowering the macromolecular degradation. Conversely, the aged handmade paper showed a similar amount of glycosidic scissions as the unaged counterpart. Carbonyl groups in the artificially aged Whatman n°1 papers seemed to increase the glycosidic scissions in the low doses range, below 0.5 kGy. Confirming previous results (Gimat et al. 2020), the optical changes appeared with considerable delay, often one year after the irradiation, and could not be directly correlated to the initial *DP* nor to the glycosidic scissions concentration that grew steadily during this post-irradiation period (dark storage, room temperature). As expected, the archival papers made of linen rags had an overall more complex X-ray exposure behavior than the model papers. Their behavior under X-ray was multifactorial and difficult to predict, whether in terms of *DP* losses (the largest being for DCN and LN1), luminescence (M and DCN exhibited the

higher luminescence intensity), or yellowing (M and LN1 yellowed the most). These observations led to the conclusion that in the samples with additives and in the aged/degraded samples, optical changes (yellowing and luminescence) were mostly uncorrelated. Moreover, as observed with the model papers, these optical changes were also not directly correlated with the macromolecular state (depolymerization). These observations underline the complex chemistry triggered by the exposure to X-rays. At very high doses (26–36 kGy), the archival papers reached the LODP immediately upon irradiation, similarly as Whatman n° 1. No color change or UV luminescence were observed within one year after the exposure at those high doses. Twenty-one months after the irradiation, two archival papers showed a slight UV luminescence. These contrasted results indicate that laboratory samples have their limitations to model archival/historic papers and that the radiochemistry at play is complex. However, the observation that, overall, the historic papers resisted better the X-ray exposures than modern papers is an important step forward that enables to consider analyzing historic papers with better confidence. This work focused on the paper material in chemical terms. Considering paper microstructure properties in the future may shed more light on the limitations encountered.

The results of this work underline the significance of studying the damage to artworks induced by X-ray technical examination. A significant outcome was to show the importance of carefully choosing the analytical conditions that limit the exposure, thus the dose, when analyzing genuine artefacts using X-rays. This can be achieved either by applying higher energy, or using low exposure times, and always maintaining some humidity in the paper, as demonstrated in our previous work. The mid-range relative humidity value recommended for paper-based cultural heritage storage is thus a good compromise. Documenting the exact location of the X-ray photons impact and implementing a long-term monitoring of the eventual changes through regular photographic follow-up under both UV and visible lights are advisable.

Acknowledgments We are grateful to synchrotron Soleil for the access to the PUMA beamline within the proposal 20181723 and to Tülin Okbinoglu for technical help on the beamline. We thank Samia Rebaa and Naomi Nganzami Ebale, undergraduate chemistry students (Sorbonne Université), for help with photography and spectroscopy. We also thank Sabrina Paris Lacombe and Oulfa Belhadj for technical help

with Size Exclusion Chromatography and Scanning Electron Microscopy, respectively.

Authors contributions Conception of the research and methodology: AG, ALD, MT, SC; PUMA Irradiation Experiment: AG, SC; physico-chemical characterizations: AG, Writing-original draft preparation: AG, ALD; Writing-review and editing: AG, ALD, MT, SC; Supervision: ALD, MT, SC.

Funding This research was supported by Paris Seine Graduate School of Humanities, Creation, Heritage, Investissements d'Avenir ANR-17-EURE-0021-Foundation for Cultural Heritage Science.

Declarations

Conflict of interest The authors declare that they have no conflict of interest.

References

- T 573 sp-15 (2015) Accelerated temperature aging of printing and writing paper by dry oven exposure apparatus. Technical Association of the Pulp and Paper Industry
- Adamo M, Brizzi M, Magaudda G et al (2001) Gamma radiation treatment of paper in different environmental conditions: chemical, physical and microbiological analysis. *Restaurator* 22:107–131
- Ahn K, Banik G, Potthast A (2012) Sustainability of mass-deacidification. part ii: evaluation of alkaline reserve. *Restaurator* 33:48–75. <https://doi.org/10.1515/res-2012-0003>
- Ahn K, Rosenau T, Potthast A (2013) The influence of alkaline reserve on the aging behavior of book papers. *Cellulose* 20:1989–2001. <https://doi.org/10.1007/s10570-013-9978-3>
- Albertin F, Astolfo A, Stampanoni M et al (2015) Ancient administrative handwritten documents: X-ray analysis and imaging. *J Synchrotron Radiat* 22:446–451. <https://doi.org/10.1107/S1600577515000314>
- Barrett T (1992) Evaluating the effect of gelatin sizing with regard to the permanence of paper. In: *The Institute of Paper Conservation: conference papers Manchester 1992*. Institute of paper conservation, Manchester, pp 228–233
- Barrow WJ (1972) *Manuscripts and documents: their deterioration and restoration*, 2nd edn. University Press of Virginia, Virginia
- Bertrand L, Schöeder S, Anglos D et al (2015) Mitigation strategies for radiation damage in the analysis of ancient materials. *TrAC Trends Anal Chem* 66:128–145. <https://doi.org/10.1016/j.trac.2014.10.005>
- Bicchieri M, Monti M, Piantanida G, Sodo A (2016) Effects of gamma irradiation on deteriorated paper. *Radiat Phys Chem* 125:21–26. <https://doi.org/10.1016/j.radphyschem.2016.03.005>
- Bouchard J, Méthot M, Jordan B (2006) The effects of ionizing radiation on the cellulose of woodfree paper. *Cellulose* 13:601–610. <https://doi.org/10.1007/s10570-005-9033-0>
- Burgess HD (1988) *Practical Considerations for Conservation Bleaching*. *JIC-CG* 13:11–26
- Carter HA (1996) The Chemistry of paper preservation: part I. the aging of paper and conservation techniques. *J Chem Educ* 73:417–420. <https://doi.org/10.1021/ed073p417>
- Castellan A, Ruggiero R, Frollini E et al (2007) Studies on fluorescence of cellulotics. *Holzforschung* 61:504–508. <https://doi.org/10.1515/HF.2007.090>
- Creagh D (2007) Chapter 1 synchrotron radiation and its use in art, archaeometry, and cultural heritage studies. *Physical Techniques in the Study of Art. Archaeology and Cultural Heritage*. Elsevier, Amsterdam, pp 1–95
- Duconseille A, Andueza D, Picard F et al (2016) Molecular changes in gelatin aging observed by NIR and fluorescence spectroscopy. *Food Hydrocoll* 61:496–503. <https://doi.org/10.1016/j.foodhyd.2016.06.007>
- Dupont A-L (2003b) Cellulose in lithium chloride/N, N-dimethylacetamide, optimisation of a dissolution method using paper substrates and stability of the solutions. *Polymer* 44:4117–4126. [https://doi.org/10.1016/S0032-3861\(03\)00398-7](https://doi.org/10.1016/S0032-3861(03)00398-7)
- Dupont A-L, Réau D, Bégin P et al (2018) Accurate molar masses of cellulose for the determination of degradation rates in complex paper samples. *Carbohydr Polym* 202:172–185. <https://doi.org/10.1016/j.carbpol.2018.08.134>
- Dupont A-L (2003a) Gelatine sizing of paper and its impact on the degradation of cellulose during ageing: a study using size-exclusion chromatography. PhD thesis. Universiteit van Amsterdam
- Emery JA, Schroeder HA (1974) Iron-catalyzed oxidation of wood carbohydrates. *Wood Sci Technol* 8:123–137. <https://doi.org/10.1007/BF00351367>
- Ershov BG (1998) Radiation-chemical degradation of cellulose and other polysaccharides. *Russ Chem Rev* 67:315. <https://doi.org/10.1070/RC1998v067n04ABEH000379>
- Evans R, Wallis AFA (1987) Comparison of cellulose molecular weights determined by high performance size exclusion chromatography and spectrometry. *Proc Fourth Int Symp Wood Pulping Chem Paris* 1:201–206
- Gervais C, Thoury M, Réguer S et al (2015) Radiation damages during synchrotron X-ray micro-analyses of Prussian blue and zinc white historic paintings: detection, mitigation and integration. *Appl Phys A* 121:949–955. <https://doi.org/10.1007/s00339-015-9462-z>
- Gimat A, Kasneryk V, Dupont A-L et al (2016) Investigating the DMPO-formate spin trapping method for the study of paper iron gall ink corrosion. *New J Chem* 40:9098–9110. <https://doi.org/10.1039/C6NJ01480A>
- Gimat A, Dupont A-L, Lauron-Pernot H et al (2017) Behavior of cellobiose in iron-containing solutions: towards a better understanding of the dominant mechanism of degradation of cellulosic paper by iron gall inks. *Cellulose* 24:5101–5115. <https://doi.org/10.1007/s10570-017-1434-3>
- Gimat A, Schöder S, Thoury M et al (2020) Short- and long-term effects of X-ray synchrotron radiation on cotton paper. *Biomacromol* 21:2795–2807. <https://doi.org/10.1021/acs.biomac.0c00512>
- Gimat A (2016) Comprehension of cellulose depolymerisation mechanisms induced by iron ions. PhD thesis. Université Pierre et Marie Curie
- Glaser L, Deckers D (2014) The Basics of fast-scanning xrf element mapping for iron-gall ink palimpsests. *Manuscr Cult* 7:104–112
- Henniges U, Hasani M, Potthast A et al (2013) Electron beam irradiation of cellulosic materials—opportunities and limitations. *Materials* 6:1584–1598. <https://doi.org/10.3390/ma6051584>

- IAEA (2016) Trends of synchrotron radiation applications in cultural heritage. Forensics and Materials Science International Atomic Energy Agency, Vienna
- Jeong M-J, Dupont A-L, de la Rie ER (2014) Degradation of cellulose at the wet–dry interface. II. Study of oxidation reactions and effect of antioxidants. *Carbohydr Polym* 101:671–683. <https://doi.org/10.1016/j.carbpol.2013.09.080>
- Kabacińska Z, Yate L, Wencka M et al (2017) Nanoscale effects of radiation (UV, X-ray, and γ) on calcite surfaces: implications for its mechanical and physico-chemical properties. *J Phys Chem C* 121:13357–13369. <https://doi.org/10.1021/acs.jpcc.7b03581.s001>
- Kocar D, Strlic M, Kolar J et al (2005) Chemiluminescence from paper III: the effect of superoxide anion and water. *Polym Degrad Stab* 88:407–414. <https://doi.org/10.1016/j.polymdegradstab.2004.12.005>
- Kozachuk M, Suda A, Ellis L et al (2016) Possible radiation-induced damage to the molecular structure of wooden artifacts due to micro-computed tomography, handheld X-ray fluorescence, and X-ray photoelectron spectroscopic techniques. *J Conserv Mus Stud* 14:2–6. <https://doi.org/10.5334/jcms.126>
- Mantler M, Klikovits J (2004) Analysis of art objects and other delicate samples: Is XRF really nondestructive? *Powder Diffr* 19:16–19. <https://doi.org/10.1154/1.1649962>
- Missori M, Righini M, Dupont A-L (2006) Gelatine sizing and discoloration: A comparative study of optical spectra obtained from ancient and artificially aged modern papers. *Opt Commun* 263:289–294. <https://doi.org/10.1016/j.optcom.2006.02.004>
- Moini M, Rollman CM, Bertrand L (2014) Assessing the impact of synchrotron X-ray irradiation on proteinaceous specimens at macro and molecular levels. *Anal Chem* 86:9417–9422. <https://doi.org/10.1021/ac502854d>
- Nevell TP (1985) Degradation of cellulose by acids, alkalis and mechanical means. Chapter 9. In: Nevell TP, Zeronian SH (eds) *Cellulose chemistry and its applications*. Ellis Horwood, Chichester, pp 223–242
- Poggi G, Sistach MC, Marin E et al (2016) Calcium hydroxide nanoparticles in hydroalcoholic gelatin solutions (GeolNan) for the deacidification and strengthening of papers containing iron gall ink. *J Cult Herit* 18:250–257. <https://doi.org/10.1016/j.culher.2015.10.005>
- Potthast A, Henniges U, Banik G (2008) Iron gall ink-induced corrosion of cellulose: aging, degradation and stabilization. Part 1: model paper studies. *Cellulose* 15:849–859. <https://doi.org/10.1007/s10570-008-9237-1>
- Pouyet E, Devine S, Grafakos T et al (2017) Revealing the biography of a hidden medieval manuscript using synchrotron and conventional imaging techniques. *Anal Chim Acta* 982:20–30. <https://doi.org/10.1016/j.aca.2017.06.016>
- Reissland B (1999) Ink corrosion aqueous and non aqueous treatment of paper objects—state of the art. *Restaurator* 20:167–180
- Röhring J, Potthast A, Rosenau T et al (2002) A novel method for the determination of carbonyl groups in celluloses by fluorescence labeling. 2. Valid Appl Biomacromol 3:969–975. <https://doi.org/10.1021/bm020030p>
- Ross-Murphy SB (1985) Properties and uses of cellulose solutions. Chapter 8. In: Nevell TP, Zeronian S (eds) *Cellulose Chemistry and its Applications*. Ellis Horwood, Chichester, pp 202–222
- Rouchon V, Belhadj O (2016) Calcium hydrogen carbonate (bicarbonate) deacidification: what you always wanted to know but never dared asking. *J Pap Conserv* 17:125–127. <https://doi.org/10.1080/18680860.2016.1287406>
- Rouchon V, Duranton M, Burgaud C et al (2011) Room-temperature study of iron gall ink impregnated paper degradation under various oxygen and humidity conditions: time-dependent monitoring by viscosity and X-ray absorption near-edge spectrometry measurements. *Anal Chem* 83:2589–2597. <https://doi.org/10.1021/ac1029242>
- Rouchon V, Belhadj O, Duranton M et al (2016) Application of Arrhenius law to DP and zero-span tensile strength measurements taken on iron gall ink impregnated papers: relevance of artificial ageing protocols. *Appl Phys A* 122:773. <https://doi.org/10.1007/s00339-016-0307-1>
- Selih VS, Strlic M, Kolar J, Pihlar B (2007) The role of transition metals in oxidative degradation of cellulose. *Polym Degrad Stab* 92:1476–1481. <https://doi.org/10.1016/j.polymdegradstab.2007.05.006>
- Sequeira S, Casanova C, Cabrita EJ (2006) Deacidification of paper using dispersions of Ca(OH)₂ nanoparticles in isopropanol. Study of Efficiency *J Cult Herit* 7:264–272. <https://doi.org/10.1016/j.culher.2006.04.004>
- Shinotsuka H, Tanuma S, Powell CJ, Penn DR (2015) Calculations of electron inelastic mean free paths. X. Data for 41 elemental solids over the 50 eV to 200 keV range with the relativistic full Penn algorithm. *Surf Interface Anal* 47:1132–1132. <https://doi.org/10.1002/sia.5861>
- T 211 om-02 (2002) Ash in wood, pulp, paper and paperboard: combustion at 525 °C. Technical Association of the Pulp and Paper Industry
- T 230 om-19 (1999) Viscosity of pulp (capillary viscometer method). Technical Association of the Pulp and Paper Industry
- T 402 sp-08 (2013) Standard conditioning and testing atmospheres for paper, board, pulp handsheets, and related products. Technical Association of the Pulp and Paper Industry
- T 509 om-15 (2002) Hydrogen ion concentration (pH) of paper extracts (cold extraction method). Technical Association of the Pulp and Paper Industry
- T 553 om-00 (2000) Alkalinity of paper as calcium carbonate (alkaline reserve of paper). Technical Association of the Pulp and Paper Industry
- T 430 cm-99 (1999) Copper Number of Pulp, Paper, and Paperboard. Technical Association of the Pulp and Paper Industry
- T 502 cm-07 (1998) Equilibrium relative humidity of paper and paperboard. Technical Association of the Pulp and Paper Industry
- Whitmore PM, Bogaard J (1994) Determination of the cellulose scission route in the hydrolytic and oxidative degradation of paper. *Restaurator* 15:26–45. <https://doi.org/10.1515/rest.1994.15.1.26>
- Yova D, Hovhannisyann V, Theodossiou T (2001) Photochemical effects and hypericin photosensitized processes in collagen. *J Biomed Opt* 6:52–57. <https://doi.org/10.1117/1.1331559>

Publisher's Note Springer Nature remains neutral with regard to jurisdictional claims in published maps and institutional affiliations.